

Synthesis, pharmacological evaluation and molecular docking of pyranopyrazole-linked 1,4-dihydropyridines as potent positive inotropes

Rakesh Kumar¹ · Neha Yadav¹ · Rodolfo Lavilla² · Daniel Blasi³ · Jordi Quintana³ · José Manuel Brea⁴ · María Isabel Loza⁴ · Jordi Mestres⁵ · Mamta Bhandari¹ · Ritu Arora¹ · Rita Kakkar¹ · Ashok K. Prasad¹

Received: 14 September 2016 / Accepted: 9 April 2017
© Springer International Publishing Switzerland 2017

Abstract 1,4-Dihydropyridines are well-known calcium channel blockers, but variations in the substituents attached to the ring have resulted in their role reversal making them calcium channel activators in some cases. We describe the microwave-assisted eco-friendly approach for the synthesis of pyranopyrazole-1,4-dihydropyridines, a new class of 1,4-DHPs, under solvent-free conditions in good yield, and screen them for various *in silico*, *in vitro* and *in vivo* activities. The *in vivo* experimentation results show that the compounds possess positive inotropic effect, and the docking results validate their good binding with calcium channels. Com-

pounds **7c**, **7g** and **7i** appear to be the most effective positive inotropes, even at low doses, and bind with the calcium channels even more strongly than Bay K 8644, a well-known calcium channel activator. The chronotropic effect for the new compounds was also studied. The target and off-target affinity profiling supported the *in vivo* results and revealed that the hybridized pyranopyrazole dihydropyridine scaffold has delivered new moderate hits, to be optimized, for the cytochrome P450 3A4 enzymes, opening avenues for combined pharmacological activity through standard structural modification.

Electronic supplementary material The online version of this article (doi:10.1007/s11030-017-9738-7) contains supplementary material, which is available to authorized users.

✉ Rakesh Kumar
rakehskp@email.com

¹ Bio-organic Laboratory, Department of Chemistry, University of Delhi, Delhi 110 007, India

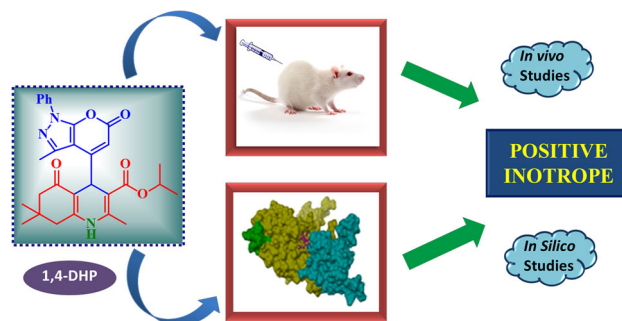
² Laboratory of Organic Chemistry, Department of Pharmacology and Therapeutical Chemistry, Faculty of Pharmacy, University of Barcelona, Barcelona Science Park, Baldiri Reixac 10-12, 08028 Barcelona, Spain

³ Drug Discovery Platform, Parc Científic de Barcelona, Baldiri Reixac 10-12, 08028 Barcelona, Spain

⁴ USEF Screening Platform, Centre of Research on Molecular Medicine and Chronic Diseases (CIMUS), Universidad de Santiago de Compostela (USC), Santiago de Compostela, Spain

⁵ Systems Pharmacology, Research Program on Biomedical Informatics (GRIB), IMIM Hospital del Mar Medical Research Institute and University Pompeu Fabra, Doctor Aiguader 88 (PRBB), 08003 Barcelona, Catalonia, Spain

Graphical Abstract



Keywords Pyranopyrazole-1 · 4-Dihydropyridines · Inotropic effect · Molecular docking · Structure–activity analysis · CYP450 inhibition · Microwave synthesis · SeO₂

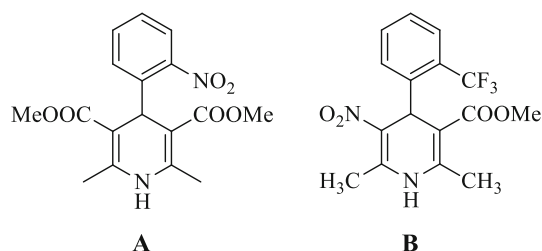
Introduction

Calcium ions are essential in various physiological signaling pathways. The movement of calcium ions across the cell occurs *via* the ligand-gated or voltage-gated calcium chan-

nels, leading to increased/decreased intracellular calcium levels generating various physiological responses [1]. The cell needs to be depolarized or excited for these channels to open up and allow the influx of calcium into the cell [2,3].

Among the various known calcium channel activators and blockers, 1,4-dihydropyridines have been observed to possess most potent binding with L-type calcium channels. 1,4-DHPs behave both as calcium channel blockers and as activators and are widely used in treating coronary heart diseases. Nifedipine (**A**) and Bay K 8644 (**B**) are well-known calcium channel blocker and activator, respectively [4].

Furthermore, 1,4-DHPs show a broad pharmacological activity profile possessing antiviral [5], antitumor [6], anti-inflammatory [7], antimicrobial [8], antitubercular [9] and antihistaminic [10] activities. 1,4-DHPs are also being explored for their binding with various receptors, namely adenosine [11,12], cannabinoid [13], adrenergic [14] and cytochrome P450 receptors [15].



With the “one-drug-one-target” paradigm, many diseases remain inadequately treated today. The failure of this protocol to treat some diseases prompted us to explore the “hybrid drugs” model, in which a compound interacts with multiple targets [16]. This strategy leads to new chemical entities with modified selectivity profiles, different or multiple modes of action and reduced side effects. The concept of hybridization impelled us to design and syn-

thesize a new class of pharmacologically active scaffolds by hybridizing two active pharmacophore units, namely 1,4-dihydropyridine analogues with the pyranopyrazole ring (Fig. 1).

Herein, we report the MW-assisted solvent-free, greener and eco-friendly approach for the synthesis of pyranopyrazole-1,4-dihydropyridine derivatives, and we report the *in vivo* results describing their effect on blood pressure and heart rate, supported by docking studies. We also report the *in silico* and *in vitro* characterization of these compounds interacting with adenosine and androgen receptors and with cytochrome P450 enzymes.

Results and discussion

Synthesis of pyranopyrazole-1,4-dihydropyridines

In this work, we have hybridized the pyrazole moiety with the pyran ring. Pyranopyrazoles are an important category of heterocyclic compounds and are widely used as parental compounds to synthesize molecules with medicinal benefits. They possess vasodilator [17], anticancer [18], analgesic [19], anti-inflammatory [20], antimicrobial [21] activities. These pyranopyrazoles are also of interest because of their structural similarity to a wide variety of flavonoids that exhibit interesting biological activities.

This vast pharmacological spectrum leads to the design of new bioactive candidates by the hybridization of the two active pharmacophore units, i.e., 1,4-dihydropyridine derivatives linked with pyranopyrazoles, as an attractive drug scaffold to evaluate their potency against hypertension and other druggable targets.

With the aim to synthesize pyranopyrazole-1,4-dihydropyridines, pyrano[2,3-*c*]pyrazole-4-carbaldehydes were first synthesized. The reaction conditions for the synthesis of the starting compounds pyrano[2,3-*c*]pyrazole-4-carbaldehydes **3a** (Scheme 1) were optimized using various parameters as given in Table 1. Various solvents were screened under microwave irradiation and conventional heating. The best yield was obtained for compounds **3a–b**, in the oxidation of compounds **2a–b** using selenium dioxide in 1,4-dioxane at reflux. The compounds **2a–b** were in turn prepared by the modified Pechmann condensation reaction of hydrazines **1a–b** with ethyl acetoacetate (**4a**) at 130–140 °C *via* the *in situ* generation of pyrazolone [22] (Scheme 1).

A series of novel pyranopyrazole-1,4-dihydropyridines **7a–l** has been synthesized following the modified Hantzsch synthesis.

The synthesis of symmetric pyranopyrazole-1,4-dihydropyridines **7a–h** was accomplished by the reaction of pyrano[2,3-*c*]pyrazole-4-carbaldehydes **3a–b**, β -keto esters

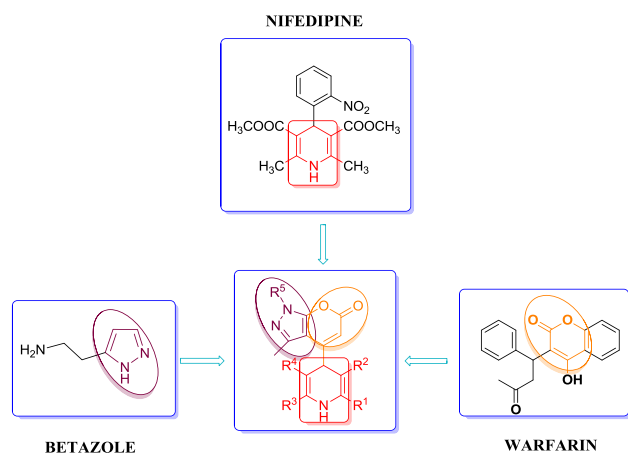
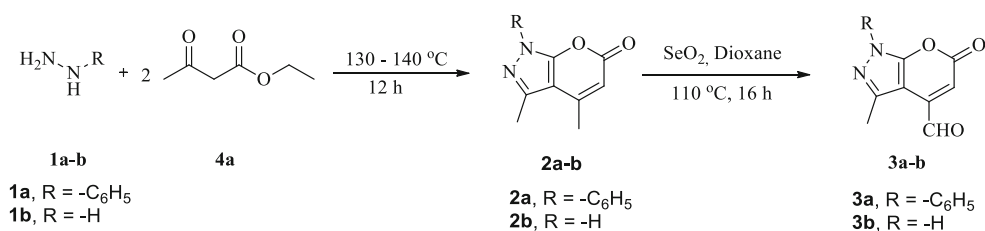


Fig. 1 Hybridization of the pyrazole, pyrano and dihydropyridine pharmacophores leading to the pyrano-pyrazole dihydropyridine compounds



Scheme 1 Synthesis of compounds **3a–b**

Table 1 Optimization of the reaction conditions for the synthesis of pyrano[2,3-*c*]pyrazole-4-carbaldehydes

Entry	Solvent	Temp (°C)	Time	Yield ^c (%)
1	Dioxane ^a	110	16 h	45
2	Xylene ^a	145	16 h	D
3	EtOH ^a	90	16 h	E
4	None ^a	120	16 h	29
5	Dioxane ^b	110	10 min	39
6	Xylene ^b	145	10 min	D
7	EtOH ^b	90	10 min	E
8	None ^b	120	10 min	30

^a Conventional heating

^b Microwave irradiation at 90 W

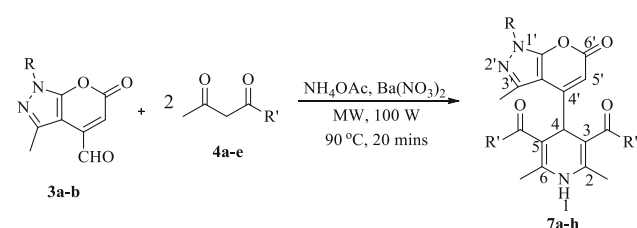
^c Isolated yields

^d Reaction yielded multiple overlapping spots on TLC difficult to isolate

^e No reaction

4a–e and ammonium acetate *via* MW irradiation under solvent-free conditions using barium nitrate as catalyst (Scheme 2), followed by a simple work-up to obtain the pure compounds. Synthesis of asymmetric pyranopyrazole-1,4-dihydropyridines **7i–k** was accomplished by the reaction of pyrano[2,3-*c*]pyrazole-4-carbaldehyde **3a**, β-keto esters **4a–c**, dimedone **5** and ammonium acetate under similar conditions. Similarly, synthesis of asymmetric pyranopyrazole-1,4-dihydropyridines **7l** was accomplished by the reaction of pyrano[2,3-*c*]pyrazole-4-carbaldehyde **3a**, methyl 3-amino crotonate **6**, β-keto ester **4c** and ammonium acetate under similar conditions (Scheme 3).

Symmetric



Scheme 2 Synthesis of compounds **7a–h**

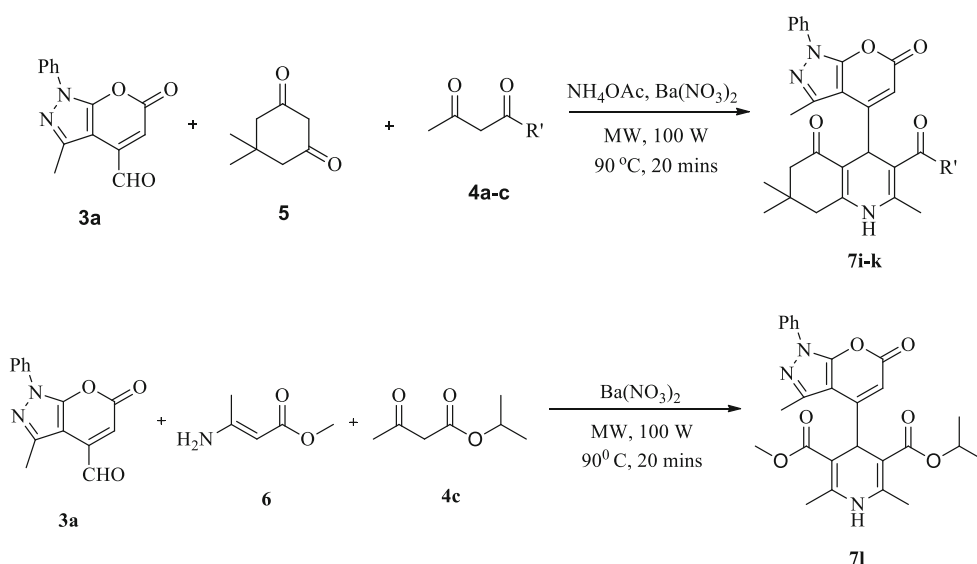
Non-symmetric

The process is versatile and allows the synthesis of symmetric DHPs and through mixed reaction of dimedone/methyl 3-amino crotonate and acetoacetic esters leads to non-symmetric derivatives as well. The transformations are selective and afford the desired compounds in useful (high) yields and purities. The details of the various compounds synthesized are depicted in Table 2. The structures of the compounds were unambiguously established based on their spectral data analysis such as ¹H NMR, ¹³C NMR, FTIR and HRMS. For all the new DHP derivatives, UPLC-MS was also performed to check their purity (see supplementary information). All the data were in good agreement to our proposed structures.

Evaluation of samples for their effect on blood pressure and heart rate

Since 1,4-dihydropyridines are primarily known to decrease the blood pressure by acting as calcium channel blockers, tracing of various hemodynamic parameters, such as HR, MAP, DBP, SBP, Rat BP in spontaneously hypertensive rats (SHR), was carried out. The effect of nifedipine (well-known dihydropyridine calcium channel blocker) and all the synthesized compounds on blood pressure and heart rate at different doses, i.e., 1, 5 and 10 mg/kg, was measured (Table 3). However, upon monitoring, the standard, as expected decreased the blood pressure, whereas, contrary to the expected results, the newly synthesized compounds appeared to be increasing the blood pressure instead of decreasing it. A graphical representation of the effect on blood pressure of different compounds at different doses is shown in Fig. 2. Compounds **7c**, **7g** and **7i** showed really good increase in BP at all three doses. Compounds **7b**, **7e**, **7h**, **7j**, **7k** and **7l** showed moderate to good increase in blood pressure at high doses (i.e., 5 and 10 mg/kg) in SHR rats. Some compounds **7c**, **7d**, **7e**, **7g**, **7h** and **7j** showed moderate increase in heart rate as well.

The *in vivo* screening showed the compounds to be acting as positive inotropes, as most of them lead to an increase in arterial blood pressure (ABP). These results thus revealed that the DHPs of this novel class were acting opposite to that of nifedipine (calcium channel blocker) and that they might



Scheme 3 Synthesis of compounds 7i–l

Table 2 Chemical structure of synthesized 1,4-dihydropyridines 7a–l

Comp. No.	Aldehyde 3	β -keto ester / β -diketone	Comp. No.	Aldehyde 3	β -keto ester/ dimedone/ methyl 3-amino crotonate
7a			7g		
7b			7h		
7c			7i		
7d			7j		
7e			7k		
7f			7l		

be acting as calcium channel activators, leading to positive inotropic effect.

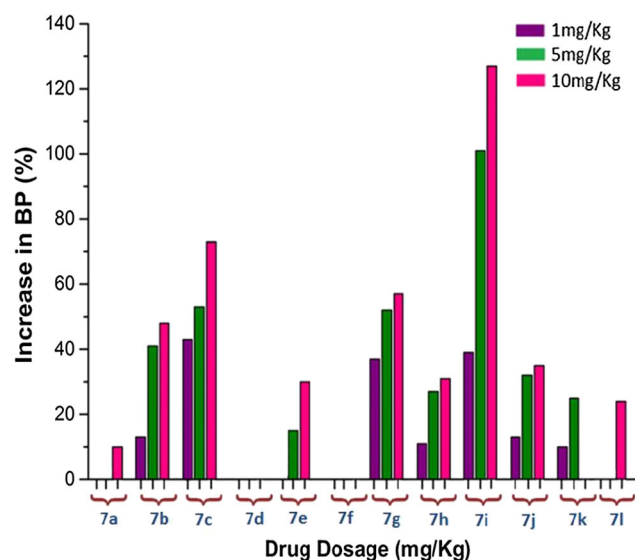
These contradictory results prompted the exploration of binding of these new 1,4-dihydropyridines with the calcium channels. Hence, we carried out docking studies to support the in vivo results.

Binding mode of the best pose into the active site of KVAP

For the theoretical studies, the experimental structures of DHP-LTCC complexes would have been good starting points for our calculations. However, owing to the large size and

Table 3 Effect on BP and heart rate

Compound	Effect on hemodynamic parameters
Nifedipine	At the dose of 1 mg/kg, it showed maximum fall of 23.5 mmHg (29.5%) within 15 min before returning to baseline after 45 min. However, there was no significant change in heart rate
7a	At 1 and 5 mg/kg, there was no significant change in BP, and at 10 mg/kg there was 10% rise in BP when compared to basal BP. It did not affect heart rate. Labored respiration was observed in animal
7b	It caused a rise of 13% at 1 mg/kg, 41% at 5 mg/kg and 48% at 10 mg/kg in BP after 15 min of drug administration. There was 14% increase in heart rate at 5 mg/kg. Labored respiration was seen in animal
7c	This compound turned milky when mixed with saline. There was 43, 53 and 73% increase in blood pressure at the doses of 1, 5 and 10 mg/kg, respectively. Increased heart rate was also observed at all three doses
7d	When this compound was mixed with saline, it turned milky. There was no effect on BP, but there was 12% rise in heart rate at 10 mg/kg
7e	At 1 mg/kg, there was no significant change in BP, but it caused a rise of 15 and 30% in BP at the doses of 5 and 10 mg/kg, respectively. There was 15% rise in heart rate at the dose of 10 mg/kg
7f	When this compound was mixed with saline, it turned milky. There was no effect on BP. There was 38% rise in heart rate at 10 mg/kg
7g	It caused a rise of 37% at 1 mg/kg, 52% at 5 mg/kg and 57% at 10 mg/kg in BP. Further, there was 11% fall in heart rate at 5 mg/kg
7h	It caused a rise of 11% at 1 mg/kg, 27% at 5 mg/kg and 31% in BP. No effect on heart rate was seen
7i	When this compound was mixed with saline, it became turbid. It caused a rise of 39% at 1 mg/kg, 101% at 5 mg/kg and 127% in BP. Heart rate at 1 mg/kg showed a fall of 5% after 15 min, but at 5 mg/kg there was 35% increase in heart rate. Labored respiration and gnawing of teeth were seen in rats
7j	After administration, this compound caused an increase of 13, 32 and 45% in BP of at the dose 1, 5 and 10 mg/kg, respectively. After the administration of 5 mg/kg, rate of respiration increased in animal. Further, there was 29% increase in heart rate
7k	When this compound was mixed with saline, it turned milky. It caused a rise of 10% at 1 mg/kg, 25% at 5 mg/kg, and there was no effect on BP at 10 mg/kg. There was 13% increase in heart rate at 1 mg/kg
7l	When this compound was mixed with saline, it became turbid. There was 24% increase at 5 mg/kg in BP. There was no effect on heart rate

**Fig. 2** Effect on blood pressure with different drug dosage. (Color figure online)

hydrophobic nature of calcium channels, the crystallographic studies on these proteins have always been a challenging task for experimentalists. Hence, a complete X-ray crystal

structure of voltage-gated Ca^{2+} channels is not available to date. Fortunately, voltage-dependent Ca^{2+} channels (KVAP) belong to the class of voltage-dependent cation (Na^+ , K^+ and Ca^{2+}) channels which allow conduction of these ions with cell membrane voltage changes. All members of this class contain six hydrophobic segments, S1–S6, per subunit, out of which the four subunits surrounding the central ion-conduction pore are identical in all these channels [23–25]. In fact, many small-molecule ligands of K^+ channels have been identified, but only a few co-crystallized with KVAP. Therefore, we first focused on determining the active site for the binding of DHPs to KVAP and then carried out docking studies using extra precision Glide (XP) available in the Schrödinger suite [26,27]. Various possible binding states were predicted by SiteMap [28], but based on their Site score and other important parameters, the active site was found to be at the interface of the two chains (A and B) of KVAP (Fig. 3). The point to note here is that this is the same site as that of binding of its inhibitor [29–31].

The Glide XP docking results are summarized in Table 4. Out of the five poses obtained, the docking score of pose 7i is found to be the best. This suggests that the ligand 7i activates the receptor more efficiently than the reference, in

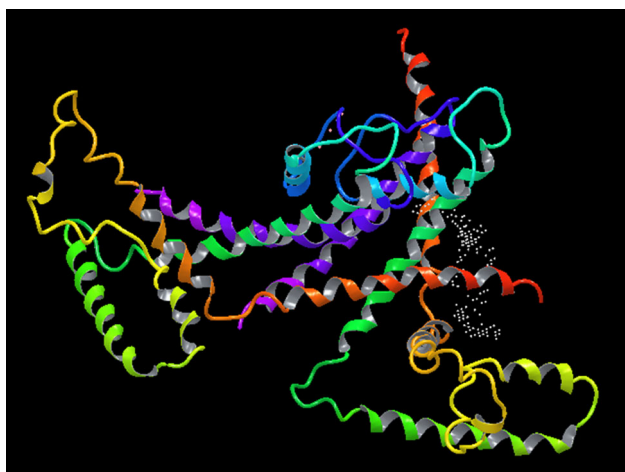


Fig. 3 Active site (white dots in protein) obtained from SiteMap

Table 4 Glide docking results of DHPs in the active site of KVAP

L#	Docking score	E_{model} /kcal/mol	Glide energy/kcal/mol
7i	-6.29	-56.42	-43.15
7c	-6.21	-44.61	-41.89
7i	-5.82	-65.47	-47.13
7g	-5.54	-57.08	-45.62
7g	-5.42	-50.69	-40.40
(S)-BAY K 8644	-5.73	-30.14	-28.08

accord with our *in vivo* results. This fact is also supported by the calculated values (Table 4) of other important scoring functions, like E_{model} and Glide energy. Therefore, the best scoring pose of **7i** was used for further analysis.

The orientation of the best pose of the most potent calcium channel activator, compound **7i**, in the active site of KVAP is shown in Fig. 4 along with its van der Waals contacts and hydrogen-bonding interactions. As can be clearly seen, the active site of the receptor comprises residues LEU 26, VAL 27, LEU 29, VAL 31 and TYR 33 of chain A and VAL 56, TYR 59, LEU 60, LEU 159, LEU 162, TYR 163 and PHE 166 of chain B, which make good contacts with ligand **7i**. A hydrogen bond with the amino acid residues of the receptor is also formed, i.e., between the hydroxyl group of TYR 163 and carbonyl oxygen of the ligand.

The active site is completely buried in a hydrophobic environment. The hydrophobic (orange) and hydrophilic (blue) maps around the active site are displayed in Fig. 5.

The observations discussed above are sufficient to estimate the potential of our compounds as activators of L-type calcium channels. Thus, by combining the results obtained by our *in vivo* and molecular docking studies, we conclude that our compound **7i** is a novel calcium channel activator and should be explored further.

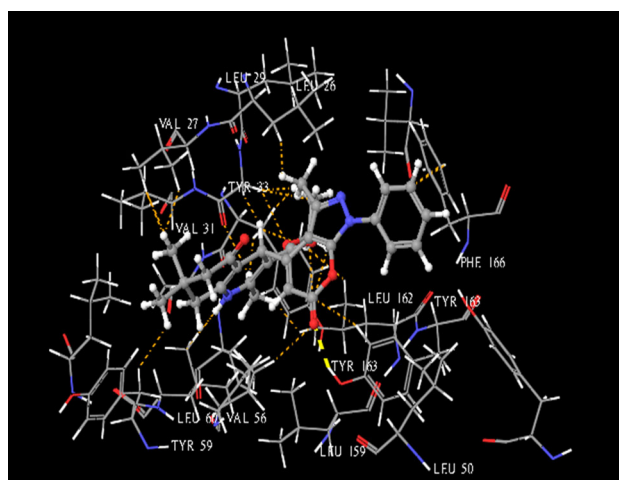


Fig. 4 Van der Waals contacts (orange dashed lines) and hydrogen-bonding interactions (yellow dashed-line) of **7i** with the residues of KVAP. (Color figure online)

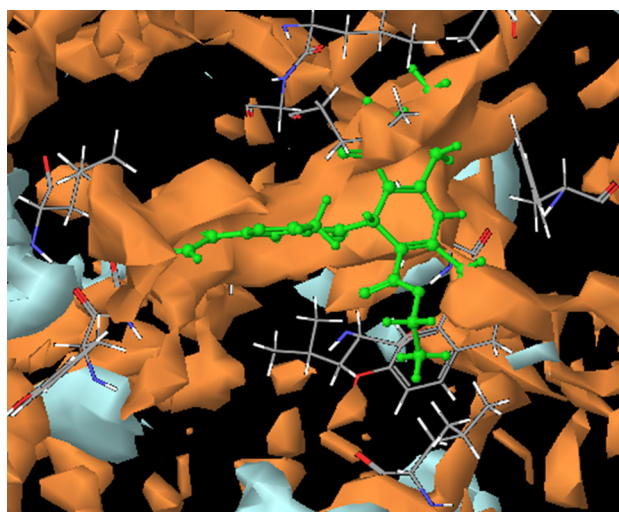


Fig. 5 L#7i (shown in green color) inside the hydrophobic (orange) and hydrophilic (blue) protein environment of KVAP. (Color figure online)

For the synthesized compounds, *in silico* and *in vitro* experiments to analyze their activity against various other targets (such as adenosine, androgen and Cyp 450 receptor) were also carried out as follows.

Structure–activity discussion

The interesting biological activity results impelled the analysis of the point of attachment of the pyranopyrazole ring in combination with the varying ester group substituents at C-3 and C-5 position of the DHP ring. The comparison of the activity results of the newly synthesized pyranopyrazole-1,4-dihydropyridines showed that the compound **7i** with nonidentical ester substitution at C-3 and C-5 and a bulky group at 4-position is the most potent out of all, in increasing

Table 5 Target and off-target affinity profiles of nifedipine (ChEMBL193) and compounds **7a–c**, **7f–g**, and **7i–j**

Compound	CACNA1C	CACNA1D	CACNA1S	AR	A1	A3	CYP3A4
Nifedipine	8.1^a 8.8	8.3^a 7.2	8.2^a 7.2	– <6.0	5.4^a <6.0	5.2^a <6.0	5.0^a <6.0
7a	– 6.2	– 7.3	– 7.7	– <6.0	– <6.0	2%^b <6.0	37%^b 6.0
7b	– 6.4	– 7.2	– 6.3	– <6.0	6%^b <6.0	1%^b <6.0	– –
7c	– 6.2	– 7.2	– 7.8	– <6.0	– <6.0	2%^b <6.0	50%^b 6.0
7f	– 7.1	– 7.2	– 8.1	16%^b/28%^c <6.0	– –	– –	– 6.2
7g	– 6.7	– 7.4	– 8.2	17%^b/31%^c 6.0	– –	– –	– <6.0
7i	– 6.7	– 6.7	– 7.6	– –	6%^b 6.1	2%^b 6.5	– <6.0
7j	– 6.8	– 7.4	– 7.6	– –	11%^b 6.3	13%^b 6.7	– –

Experimental values are highlighted in bold, whereas predicted pK_i values (in μM) (obtained from CT-link [32,33]) are given in italics

^a Average pK_i values from ChEMBL [34]

^b %Inhibition at 10 μM

^c %Inhibition at 100 μM

Target abbreviations: CACNA1C, Voltage-dependent L-type calcium channel subunit alpha-1C; CACNA1D, Voltage-dependent L-type calcium channel subunit alpha-1D; CACNA1S, Voltage-dependent L-type calcium channel subunit alpha-1S; AR, androgen receptor; A1, adenosine A1 receptor; A3, adenosine A3 receptor; CYP3A4, cytochrome P450 3A4

the BP. This is followed by compounds **7c** and **7g**. DHPs **7c** and **7g** with identical ester substituent showed maximum activity with the presence of *i*-propyl ester substituent as compared to the less bulky ethyl and methyl ester substituents. However, the activity decreased or was completely lost when the *i*-propyl ester was replaced with the benzyl ester in **7h** and **7d**. When the dimedone ring in **7i** was replaced with the ethyl ester substituent yielding a symmetrical DHP (**7a**), the complete loss of activity was observed.

On comparing the effect of *N*-phenyl pyranopyrazole and unsubstituted pyranopyrazole at 4-position, it appeared that *N*-substituted pyranopyrazole yielded compounds with better activity, with exception of benzyl ester substituents at the 3rd and 5th position, presumably because of the steric hindrance due to bulky groups.

Off-target pharmacology: computational prediction and experimental validation

An integrated combination of ligand-based approaches, as implemented in the software CT-link [32,33], were used to estimate the target and off-target pharmacology of nifedipine and compounds **7a–c**, **7f–g**, and **7i–j**. The results are collected in Table 5.

Nifedipine is known to bind with potent affinity (<10 nM) to the voltage-dependent L-type calcium channel subunits

alpha-1C (CACNA1C), alpha-1D (CACNA1D), and alpha-1S (CACNA1S) [34]. For these three targets, affinities (pK_i) were predicted within 1 log unit of the respective experimental values. In addition, nifedipine is also known to have weak off-target affinities for the adenosine A1 and A3 receptors and the cytochrome P450 3A4 (CYP3A4) [34]. Indeed, predicted pK_i values for those three off-targets were above 1 micromolar ($pK_i < 6.0$). Finally, nifedipine was also predicted to have weak off-target affinities for several nuclear receptors, the androgen receptor (AR) being among them. Even though experimental binding affinities between nifedipine and nuclear receptors are currently lacking in publicly available databases [34], the antagonistic effect of nifedipine on the mineralocorticoid receptor has been reported [35], and thus, nuclear receptors also deserve some consideration as weak off-targets of this drug.

Taking the target and off-target pharmacology of nifedipine as reference, the corresponding predicted affinities for compounds **7a–c**, **7f–g**, and **7i–j** were also obtained (Table 5). As can be observed, all seven 1,4-DHPs are predicted to bind to the same three L-type calcium channel targets of nifedipine, which would substantiate their effect on blood pressure and heart rate (*vide supra*).

Moreover, weak micromolar affinities for the off-targets of nifedipine were also predicted for some of the compounds.

For example, compounds **7a–c** and **7i–j** were predicted to have affinity for the adenosine A1 and A3 receptors. Unfortunately, in vitro testing of the five compounds on those two off-targets did not result in any relevant affinity. Also, compounds **7a**, **7c** and **7f–g** were predicted to have affinity for the androgen receptor. However, in vitro testing of compounds **7f–g** on that off-target returned only very weak affinities. Finally, compounds **7a**, **7c**, **7f–g** and **7i** were predicted to be weak binders of CYP3A4. In this case, in vitro testing of compounds **7a** and **7c** on this key enzyme for drug metabolism did confirm weak micromolar affinity binding.

Conclusion

A new class of 1,4-dihydropyridines containing the pyranopyrazole moiety was successfully synthesized and screened for various in silico, in vitro and in vivo activities. The in vivo experimentation results show that most of the compounds of this novel class of 1,4-DHPs act as potent positive inotropes, as they lead to an increase in arterial blood pressure (ABP). Compounds **7c**, **7g** and **7i** appear to be the most effective positive inotropes, even at low doses.

Some of them caused moderate increase in the heart rate as well. The docking results for these compounds were also in agreement with the in vivo results. Based on the in vivo and docking experiments, compound **7i** appeared to be the most potent positive inotrope. The docking results showed that compound **7i** possesses stronger binding than the standard BAY K 8644 with the calcium channel. The positive inotropic effect of these compounds might be attributed to the attachment of pyranopyrazole ring at the 4-position of 1,4-DHP ring. The compounds can be further investigated for their effects on BP in normotensive rats and their binding with calcium channel, to confirm the mechanistic pathway for the positive inotropic activity.

The target and off-target affinity profiles of nifedipine (ChEMBL193) and compounds **7a–c**, **7f–g**, and **7i–j** show that the compounds are predicted to bind with the three L-type calcium channel targets quite strongly like nifedipine, hence altering the blood pressure and heart rate. Also, these affinity profiles revealed that the hybridized dihydropyridine–pyranopyrazole scaffold has delivered new moderate hits, to be optimized, for the cytochrome P450 3A4 receptors, opening avenues for combined pharmacological activity through standard structural modification.

Experimental

Materials and methods

All chemicals used in the synthesis of 1,4-dihydropyridine analogues were purchased from Sigma-Aldrich, Fluka, and

some local suppliers, and were used as such without any prior purification. Homogeneity of all the products was analyzed by thin-layer chromatography (TLC) on alumina-coated plates (Merck). Product samples in MeOH were loaded on TLC plates and developed in CHCl₃–MeOH (9.5:0.5, v/v). UV radiation was used as the visualizing agent. Compounds were purified by column chromatography on silica gel columns (100–200 mesh size, CDH), using petroleum ether–ethyl acetate (3:2, v/v) as the eluent. Melting points were determined in open glass capillary tubes on a Buchi M-560 instrument and are uncorrected. Infrared (IR) spectra were recorded in KBr medium using a PerkinElmer Fourier Transform-IR spectrometer, whereas ¹H and ¹³C nuclear magnetic resonance (NMR) spectra were recorded in DMSO-*d*₆ and CDCl₃ medium on a JNM ECX-400P (JEOL, USA) spectrometer with tetramethylsilane (TMS) as internal reference and recorded in ppm. IR and NMR spectra were recorded at the Department of Chemistry and USIC, University of Delhi, India. HRMS data were collected on high-resolution EI-mass spectrometer with a resolution of 10,000 on 6530 QTOF LCMS, at University Scientific Instrument Center (USIC), University of Delhi, Delhi, India. Absorption frequencies (ν) are expressed in cm⁻¹, chemical shifts in ppm (δ -scale) and coupling constants (J) in Hz. Splitting patterns are described as singlet (s), doublet (d) and multiplet (m). All the experiments in microwave were carried out in a closed vial applying a dedicated CEM-Discover monomode microwave apparatus operating at a frequency of 2.45 GHz with continuous irradiation power from 0 to 300 W (CEM Corporation).

Synthesis

General procedure for the synthesis of 3,4-dimethylpyrano[2,3-c]pyrazol-6(1H)-one, 2a–b

A well-stirred mixture of phenylhydrazine **1a**/hydrazine hydrate **1b** (0.14 mol) and ethyl acetoacetate **4a** (0.28 mol) was heated for 12 h at 130–140 °C with continuous stirring, and the progress of the reaction was monitored by TLC. After completion of the reaction, the reaction mixture was allowed to cool down to room temperature and washed with diethyl ether (5 × 150 mL). A yellowish crystalline solid was obtained as pure solid.

3-Methyl-6-oxo-1-phenyl-1,6-dihydropyrano[2,3-c]pyrazole-4-carbaldehyde, 3a

To a stirred solution of 3,4-dimethyl-1-phenylpyrano[2,3-c]pyrazol-6(1H)-one **2a** (20 g, 0.08 mol) in 1,4-dioxane was added SeO₂ (0.14 mol) and the reaction mixture was refluxed for 16 h. The progress of the reaction was monitored by TLC, and it was allowed to attain room temperature after

the complete conversion of the reactant. The deposited selenium metal was filtered off, and the residue was washed with ethyl acetate (2–3 times). The filtrate was concentrated *in vacuo*, and the obtained residue was purified using silica gel column chromatography petroleum ether-ethyl acetate (3:2, v/v) to obtain pure product as a yellow colored solid in 45 % yield. Melting Point 154–156 °C; IR (KBr) ν_{\max} : (cm⁻¹) 1709, 1688, 1604, 1478; ¹H NMR (400 MHz, CDCl₃) δ 9.99 (1H, s, -CHO), 7.82 (2H, d, *J* = 7.32 Hz, Ar-H), 7.51–7.47 (2H, m, Ar-H), 7.37–7.33 (1H, m, Ar-H), 6.49 (1H, s, H-5), 2.63 (3H, s, -CH₃); ¹³C NMR (100 MHz, DMSO) 191.85, 159.68, 159.10, 151.10, 145.39, 136.48, 136.22, 129.52, 127.54, 120.99, 114.22, 15.90; HRMS: Calculated for [M + H]⁺ 255.0770, found 255.0761.

3-Methyl-6-oxo-1,6-dihydropyrano[2,3-c]pyrazol-4-carbaldehyde, 3b

Compound **3b** was prepared from 3,4-dimethylpyrano[2,3-c]pyrazol-6(1H)-one **2a** (20 g, 0.08 mol) using the procedure described for **3a**. Yield 55 %; Yellow colored solid; melting point 162–164 °C; IR (KBr) ν_{\max} : (cm⁻¹) 3222, 1701, 1692, 1601; ¹H NMR (400 MHz, DMSO) δ 13.15 (1H, s, -NH), 9.86 (1H, s, -CHO), 6.69 (1H, s, H-5), 2.44 (3H, s, -CH₃); ¹³C NMR (100 MHz, DMSO) δ 192.63, 161.92, 161.32, 155.58, 145.08, 137.63, 117.86, 13.05; HRMS: Calculated for [M + H]⁺ 179.0457, found 179.0459.

Diethyl 2,6-dimethyl-4-(3-methyl-6-oxo-1-phenyl-1,6-dihydropyrano[2,3-c]pyrazol-4-yl)-1,4-dihydropyridine-3,5-dicarboxylate, 7a

A mixture of 3-methyl-6-oxo-1-phenyl-1,6-dihydropyrano[2,3-c]pyrazole-4-carbaldehyde **3a** (1 g, 0.004 mol), ethyl acetoacetate **4a** (0.008 mol), ammonium acetate (0.006 mol) and barium nitrate (2 mol%) was irradiated at 90 °C for 20 min at 100 W power in a microwave synthesizer. The reaction mixture was allowed to attain room temperature after the complete conversion of the reactant as monitored by TLC. The reaction mixture was poured into ethanol, and the solid obtained was washed with cold water. The desired product was obtained as an off-white solid in 75% yield. Melting Point 297–299 °C; IR (KBr) ν_{\max} : (cm⁻¹) 3241, 2963, 1754, 1698, 1574, 1383, 1220, 774; ¹H NMR (400 MHz, DMSO) δ 8.94 (1H, s, -NH), 7.74 (2H, d, *J* = 7.69 Hz, Ar-H), 7.54–7.51 (2H, m, Ar-H), 7.37–7.34 (1H, m, Ar-H), 5.77 (1H, s, H-5'), 5.03 (1H, s, H-4), 3.97–3.91 (4H, m, -OCH₂CH₃), 2.66 (3H, s, H-3'), 2.25 (6H, s, H-2 & 6), 0.96 (6H, m, -OCH₂CH₃); ¹³C NMR (100 MHz, DMSO) δ 168.34, 166.64, 166.13, 149.12, 146.35, 145.71, 136.53, 129.57, 127.03, 120.66, 105.11, 102.17, 101.65, 59.45, 36.00, 18.64, 15.15, 13.99; HRMS: Calculated for [M + H]⁺ 478.1976, found 478.1970.

Dimethyl 2,6-dimethyl-4-(3-methyl-6-oxo-1-phenyl-1,6-dihydropyrano[2,3-c]pyrazol-4-yl)-1,4-dihydropyridine-3,5-dicarboxylate, 7b

Compound **7b** was prepared from **3a** (1 g, 0.004 mol), methyl acetoacetate **4b** (0.008 mol) using the procedure described for **7a**. Yield 752%; off-white solid; melting point 288–290 °C; IR (KBr) ν_{\max} : (cm⁻¹) 3200, 2947, 1748, 1709, 1549, 1381, 1210, 768; ¹H NMR (400 MHz, CDCl₃) δ 7.86 (2H, d, *J* = 7.79 Hz, Ar-H), 7.48–7.44 (2H, m, Ar-H), 7.32–7.28 (1H, m, Ar-H), 6.00 (1H, s, H-5'), 5.87 (1H, br, -NH), 5.12 (1H, s, H-4), 3.59 (6H, s, -OCH₃), 2.76 (3H, s, H-3'), 2.34 (6H, s, H-2 & 6); ¹³C NMR (100 MHz, DMSO) δ 168.61, 167.48, 160.71, 149.52, 147.09, 145.94, 136.77, 129.95, 127.70, 121.05, 105.44, 102.20, 101.86, 51.25, 38.87, 18.73, 14.97; HRMS: Calculated for [M + H]⁺ 450.1660, found 450.1651.

Diisopropyl 2,6-dimethyl-4-(3-methyl-6-oxo-1-phenyl-1,6-dihydropyrano[2,3-c]pyrazol-4-yl)-1,4-dihydropyridine-3,5-dicarboxylate, 7c

Compound **7c** was prepared from **3a** (1 g, 0.004 mol), isopropyl acetoacetate **4c** (0.008 mol) using the procedure described for **7a**. Yield 70%; off-white solid; melting point 268–270 °C; IR (KBr) ν_{\max} : (cm⁻¹) 3286, 2980, 1774, 1743, 1551, 1384, 1221, 772; ¹H NMR (400 MHz, DMSO) δ 8.85 (1H, s, -NH), 7.72 (2H, d, *J* = 7.93 Hz, Ar-H), 7.54–7.50 (2H, m, Ar-H), 7.37–7.34 (1H, m, Ar-H), 5.76 (1H, s, H-5'), 4.95 (1H, s, H-4), 4.83–4.80 (2H, m, -CH(CH₃)₂), 2.69 (3H, s, H-3'), 2.22 (6H, s, H-2 & 6), 1.08 (6H, d, *J* = 6.10 Hz, -OCH(CH₃)₂), 0.87 (6H, d, *J* = 6.10 Hz, -OCH(CH₃)₂); ¹³C NMR (100 MHz, DMSO) δ 168.68, 166.33, 160.39, 149.06, 146.07, 136.56, 129.68, 127.29, 120.72, 104.96, 102.67, 101.85, 66.83, 36.24, 21.74, 21.27, 18.89, 18.69, 15.77; HRMS: Calculated for [M + H]⁺ 506.2286, found 506.2283.

Dibenzyl 2,6-dimethyl-4-(3-methyl-6-oxo-1-phenyl-1,6-dihydropyrano[2,3-c]pyrazol-4-yl)-1,4-dihydropyridine-3,5-dicarboxylate, 7d

Compound **7d** was prepared from **3a** (1 g, 0.004 mol), benzyl acetoacetate **4d** (0.008 mol) using the procedure described for **7a**. Yield 75%; off-white solid; melting point 252–254 °C; IR (KBr) ν_{\max} : (cm⁻¹) 3293, 2957, 1711, 1676, 1599, 1382, 1210, 758; ¹H NMR (400 MHz, DMSO) δ 9.05 (1H, s, -NH), 7.70 (2H, d, *J* = 7.93 Hz, Ar-H), 7.59–7.55 (2H, m, Ar-H), 7.41–7.37 (1H, m, Ar-H), 7.12–7.10 (6H, m, Ar-H), 7.01–6.99 (4H, m, Ar-H), 5.76 (1H, s, H-5'), 5.17 (2H, d, *J* = 12.21 Hz, -OCH₂), 5.10 (1H, s, H-4), 4.81 (2H, d, *J* = 12.21 Hz, -OCH₂), 2.45 (3H, s, H-3'), 2.28 (6H, s, H-2 & 6); ¹³C NMR (100 MHz, DMSO)

δ 168.47, 166.32, 160.10, 148.77, 146.95, 145.32, 136.21, 129.47, 128.07, 127.67, 126.97, 120.38, 105.12, 102.41, 101.41, 64.82, 35.95, 18.65, 14.78; HRMS: Calculated for $[M + H]^+$ 602.2286, found 602.2278.

1,1-(2,6-Dimethyl-4-(3-methyl-6-oxo-1-phenyl-1,6-dihydropyrano[2,3-c]pyrazol-4-yl)-1,4-dihydropyridine-3,5-diyl)diethanone, 7e

Compound **7e** was prepared from **3a** (1 g, 0.004 mol), acetylacetone **4e** (0.008 mol) using the procedure described for **7a**. Yield 70%; off-white solid; melting point 283–285 °C; IR (KBr) ν_{\max} (cm⁻¹) 3200, 2840, 1710, 1577, 1380, 1220, 793; ¹H NMR (400 MHz, DMSO) δ 8.99 (1H, s, -NH), 7.74 (2H, d, $J = 7.32$ Hz, Ar-H), 7.56–7.52 (2H, m, Ar-H), 7.39–7.35 (1H, m, Ar-H), 5.66 (1H, s, H-5'), 5.03 (1H, s, H-4), 2.84 (3H, s, H-3'), 2.36 (6H, s, -COCH₃), 2.26 (6H, s, H-2 & 6); ¹³C NMR (100 MHz, DMSO) δ 195.53, 168.43, 160.24, 149.04, 146.62, 145.70, 136.60, 129.52, 127.11, 120.79, 114.97, 103.96, 102.61, 36.03, 31.51, 19.65, 15.61; HRMS: Calculated for $[M + H]^+$ 418.1768, found 418.1762.

Dimethyl 2,6-dimethyl-4-(3-methyl-6-oxo-1,6-dihydropyrano[2,3-c]pyrazol-4-yl)-1,4-dihydropyridine-3,5-dicarboxylate, 7f

Compound **7f** was prepared from **3b** (1 g, 0.004 mol), methyl acetoacetate **4b** (0.008 mol) using the procedure described for **7a**. Yield 72%; off-white solid; melting point 269–271 °C; IR (KBr) ν_{\max} (cm⁻¹) 3229, 2952, 1688, 1599, 1502; ¹H NMR (400 MHz, DMSO) δ 12.97 (1H, s, -NH), 8.96 (1H, s, -NH), 5.69 (1H, s, H-5'), 4.98 (1H, s, H-4), 3.46 (6H, s, -OCH₃), 2.64 (3H, s, H-3'), 2.26 (6H, s, H-2 & 6); ¹³C NMR (100 MHz, DMSO) δ 167.08, 166.79, 162.50, 158.86, 146.42, 137.68, 107.42, 101.56, 100.18, 50.85, 35.69, 18.42, 11.82; HRMS: Calculated for $[M + H]^+$ 374.1360, found 374.1359.

Diisopropyl 2,6-dimethyl-4-(3-methyl-6-oxo-1,6-dihydropyrano[2,3-c]pyrazol-4-yl)-1,4-dihydropyridine-3,5-dicarboxylate, 7g

Compound **7g** was prepared from **3b** (1 g, 0.004 mol), isopropyl acetoacetate **4c** (0.008 mol) using the procedure described for **7a**. Yield 73%; off-white solid; melting point 236–238 °C; IR (KBr) ν_{\max} (cm⁻¹) 3222, 2979, 2933, 1696, 1674, 1598; ¹H NMR (400 MHz, DMSO) δ 12.95 (1H, s, -NH), 8.81 (1H, s, -NH), 5.67 (1H, s, H-5'), 4.89 (1H, s, H-4), 4.86–4.80 (2H, m, -CH(CH₃)₂), 2.69 (3H, s, H-3'), 2.24 (6H, s, H-2 & 6), 1.08 (6H, d, $J = 6.10$ Hz, -OCH(CH₃)₂), 0.87 (6H, d, $J = 6.10$ Hz, -OCH(CH₃)₂); ¹³C NMR (100 MHz, DMSO) δ 166.50, 162.63, 161.40, 152.72, 145.75, 138.10, 137.09, 107.30, 106.87, 66.72, 21.72, 21.26,

18.80, 11.40; HRMS: Calculated for $[M + H]^+$ 430.1979, found 430.1970.

Dibenzyl 2,6-dimethyl-4-(3-methyl-6-oxo-1,6-dihydropyrano[2,3-c]pyrazol-4-yl)-1,4-dihydropyridine-3,5-dicarboxylate, 7h

Compound **7h** was prepared from **3b** (1 g, 0.004 mol), benzyl acetoacetate **4d** (0.008 mol) using the procedure described for **7a**. Yield 72%; off-white solid; melting point 203–205 °C; IR (KBr) ν_{\max} (cm⁻¹) 3221, 3031, 2359, 1698, 1601, 1498, 1213; ¹H NMR (400 MHz, DMSO) δ 12.95 (1H, s, -NH), 9.01 (1H, s, -NH), 7.23–7.21 (6H, m, Ar-H), 7.04–7.02 (4H, m, Ar-H), 5.69 (1H, s, H-5'), 5.05–4.90 (5H, m, -OCH₂ & H-4), 2.47 (3H, s, H-3'), 2.26 (6H, s, H-2 & 6); ¹³C NMR (100 MHz, DMSO) δ 166.85, 166.57, 162.66, 161.45, 159.12, 152.77, 146.82, 137.12, 136.35, 128.55, 128.50, 128.35, 128.19, 127.96, 127.77, 107.46, 106.90, 101.55, 100.62, 65.24, 35.70, 18.80, 11.43; HRMS: Calculated for $[M + H]^+$ 526.1977, found 526.1977.

Ethyl 2,7,7-trimethyl-4-(3-methyl-6-oxo-1-phenyl-1,6-dihydropyrano[2,3-c]pyrazol-4-yl)-5-oxo-1,4,5,6,7,8-hexahydroquinoline-3-carboxylate, 7i

A mixture of 3-methyl-6-oxo-1-phenyl-1,6-dihydropyrano[2,3-c]pyrazole-4-carbaldehyde **3a** (1 g, 0.004 mol), dimedone **5**, ethyl acetoacetate **4a** (0.008 mol), ammonium acetate (0.006 mol) and barium nitrate (2 mol%) was irradiated at 90 °C for 20 min at 100 W power in a microwave synthesizer. The reaction mixture was allowed to attain room temperature after the complete conversion of the reactant as monitored by TLC. The reaction mixture was poured into ethanol, and the solid obtained was washed with cold water. The desired product was obtained as an off-white solid in 71% yield. Melting point 308–310 °C; IR (KBr) ν_{\max} (cm⁻¹) 3193, 2976, 1739, 1694, 1549, 1375, 1221, 770; ¹H NMR (400 MHz, DMSO) δ 9.27 (1H, s, -NH), 7.77 (2H, d, $J = 7.79$ Hz, Ar-H), 7.56–7.52 (2H, m, Ar-H), 7.39–7.35 (1H, m, Ar-H), 5.67 (1H, s, H-5'), 5.05 (1H, s, H-4), 4.00–3.89 (2H, m, -OCH₂CH₃), 2.77 (3H, s, H-3'), 2.45–2.35 (2H, m, -CH₂), 2.32 (3H, s, H-2), 2.20 (1H, d, $J = 16.03$ Hz, -CH₂), 2.01 (1H, d, $J = 16.03$ Hz, -CH₂), 1.01 (3H, s, -C(CH₃)₂), 0.95–0.92 (3H, m, -OCH₂CH₃), 0.89 (3H, s, -C(CH₃)₂); ¹³C NMR (100 MHz, DMSO) δ 194.86, 167.72, 166.48, 160.25, 150.27, 149.15, 146.46, 146.23, 136.58, 129.61, 127.23, 120.72, 109.96, 104.55, 103.13, 102.63, 59.56, 49.97, 33.49, 32.30, 28.90, 26.56, 18.63, 15.49, 13.87; HRMS: Calculated for $[M + H]^+$ 488.2193, found 488.2194.

Methyl 2,7,7-trimethyl-4-(3-methyl-6-oxo-1-phenyl-1,6-dihydropyrano[2,3-c]pyrazol-4-yl)-5-oxo-1,4,5,6,7,8-hexahydroquinoline-3-carboxylate, 7j

Compound **7j** was prepared from **3a** (1 g, 0.004 mol), methyl acetoacetate **4b** (0.008 mol) using the procedure described for **7i**. Yield 75%; off-white solid; melting point 295–297 °C; IR (KBr) ν_{\max} (cm⁻¹) 3184, 2975, 1746, 1701, 1563, 1381, 1238, 768; ¹H NMR (400 MHz, DMSO) δ 9.28 (1H, s, -NH), 7.78 (2H, d, *J* = 7.33 Hz, Ar-H), 7.56–7.52 (2H, m, Ar-H), 7.39–7.36 (1H, m, Ar-H), 5.67 (1H, s, H-5'), 5.07 (1H, s, H-4), 3.47 (3H, s, -OCH₃), 2.76 (3H, s, H-3'), 2.46–2.35 (2H, s, -CH₂), 2.32 (3H, s, H-2), 2.20 (1H, d, *J* = 16.03 Hz, -CH₂), 2.02 (1H, d, *J* = 16.03 Hz, -CH₂), 1.01 (3H, s, -C(CH₃)₂), 0.90 (3H, s, -C(CH₃)₂); ¹³C NMR (100 MHz, DMSO) δ 195.13, 167.69, 167.13, 160.44, 150.49, 149.31, 146.70, 146.23, 136.68, 129.72, 127.35, 120.79, 110.21, 104.70, 103.10, 102.54, 51.07, 50.04, 33.56, 32.44, 29.09, 26.57, 18.66, 15.31; HRMS: Calculated for [M + H]⁺ 474.2030, found 474.2035.

Isopropyl 2,7,7-trimethyl-4-(3-methyl-6-oxo-1-phenyl-1,6-dihydropyrano[2,3-c]pyrazol-4-yl)-5-oxo-1,4,5,6,7,8-hexahydroquinoline-3-carboxylate, 7k

Compound **7k** was prepared from **3a** (1 g, 0.004 mol), isopropyl acetoacetate **4c** (0.008 mol) using the procedure described for **7i**. Yield 68%; off-white solid; melting point 292–294 °C; IR (KBr) ν_{\max} (cm⁻¹) 3215, 2991, 1789, 1711, 1589, 1393, 1241, 772; ¹H NMR (400 MHz, DMSO) δ 9.23 (1H, s, -NH), 7.76 (2H, d, *J* = 7.93 Hz, Ar-H), 7.56–7.52 (2H, m, Ar-H), 7.39–7.36 (1H, m, Ar-H), 5.67 (1H, s, H-5'), 5.01 (1H, s, H-4), 4.86–4.80 (1H, m, -CH(CH₃)₂), 2.78 (3H, s, H-3'), 2.44–2.34 (2H, m, -CH₂), 2.32 (3H, s, H-2), 2.18 (1H, d, *J* = 15.87 Hz, -CH₂), 2.01 (1H, d, *J* = 16.03 Hz, -CH₂), 1.09 (3H, d, *J* = 6.10 Hz, -OCH(CH₃)₂), 1.00 (3H, s, -C(CH₃)₂), 0.89 (3H, s, -C(CH₃)₂), 0.76 (3H, d, *J* = 6.10 Hz, -OCH(CH₃)₂); ¹³C NMR (100 MHz, DMSO) δ 194.71, 167.82, 165.89, 160.16, 150.14, 149.05, 146.28, 146.22, 136.51, 129.55, 127.16, 120.68, 109.79, 104.43, 103.30, 102.81, 66.55, 49.95, 33.49, 32.18, 28.72, 26.60, 21.63, 20.91, 18.65, 15.73; HRMS: Calculated for [M + H]⁺ 502.2349, found 502.2344.

Isopropyl 5-acetyl-2,6-dimethyl-4-(3-methyl-6-oxo-1-phenyl-1,6-dihydropyrano[2,3-c]pyrazol-4-yl)-1,4-dihydropyridine-3-carboxylate, 7l

A mixture of 3-methyl-6-oxo-1-phenyl-1,6-dihydropyrano[2,3-c]pyrazole-4-carbaldehyde **3a** (1 g, 0.004 mol), methyl 3-amino crotonate **6** (0.006 mol), isopropyl acetoacetate **4c** (0.008 mol) and barium nitrate (2 mol%) was irradiated at 90 °C for 20 min at 100 W power in a microwave synthesizer.

The reaction mixture was allowed to attain room temperature after the complete conversion of the reactant as monitored by TLC. The reaction mixture was poured into ethanol, and the solid obtained was washed with cold water. The desired product was obtained as an off-white solid in 62% yield. Melting Point 253–255 °C; IR (KBr) ν_{\max} : (cm⁻¹) 3210, 2981, 1748, 1689, 1550, 1335, 1220, 772; ¹H NMR (400 MHz, DMSO) δ 9.11 (1H, s, -NH), 7.77 (2H, d, *J* = 5.49 Hz, Ar-H), 7.57–7.53 (2H, m, Ar-H), 7.40–7.38 (1H, m, Ar-H), 5.80 (1H, s, H-5'), 5.03 (1H, s, H-4), 4.88–4.82 (1H, m, -OCH(CH₃)₂), 3.48 (1H, s, H-4), 2.70 (3H, s, H-3'), 2.27 (6H, s, H-2), 1.11 (3H, d, *J* = 6.10 Hz, -OCH(CH₃)₂), 0.87 (3H, d, *J* = 6.10 Hz, -OCH(CH₃)₂); ¹³C NMR (100 MHz, DMSO) δ 168.56, 167.26, 166.39, 160.39, 149.26, 146.71, 146.26, 145.86, 136.61, 129.73, 127.41, 120.82, 105.17, 102.35, 102.17, 101.38, 66.89, 50.94, 36.12, 21.80, 21.25, 18.82, 18.66, 15.37; HRMS: Calculated for [M + H]⁺ 478.1978, found 478.1972.

Biological evaluation

Blood pressure and heart rate monitoring

Male spontaneously hypertensive rats (200–300 g), obtained from animal house, CSIR-Central Drug Research Institute (CSIR-CDRI), were maintained under standard conditions of 12-h/12-h light-dark cycle and temperature (23 ± 2 °C). The animals were housed in cages and provided free access to food (standard pellet chow) and water. The animals were handled according to the guidelines of Committee for the Purpose of Control and Supervision of Experiments on Animals (CPCSEA), India, and Institutional Animal Ethics Committee of CSIR-CDRI. These animals were used to study the antihypertensive potential of the compounds.

Measurement of hemodynamic parameters

The animals were weighed and anaesthetized for surgery with urethane (Sigma, USA) administered intraperitoneally (i.p.) at the dose of 1.25 g/kg. The trachea was cannulated with polyethylene tube for respiration. For measurement of blood pressure (BP) and heart rate (HR), the left carotid artery was cannulated with a pressure transducer which was connected with a data acquisition system (AD Instruments, Australia). The right external jugular vein was cannulated for the administration of drugs.

Preparation and administration of nifedipine and compounds

Standard calcium channel blocker nifedipine was dissolved in polyethylene glycol 400 and was administered at the dose of 1 mg/kg intravenously (i.v.) in a constant volume of 0.5 mL

over a period of 10–15 s. The venous catheter was then flushed with an additional 0.2 mL of saline. The compounds were solubilized in 100% DMSO and were administered at the doses of 1, 5 and 10 mg/kg through i.v. route in a constant volume of 0.5 mL over a period of 10–15 s, and the venous catheter was then flushed with an additional 0.2 mL of saline.

Molecular docking studies

The work is divided into three steps as follows:

Step 1: Preparation of ligand library of synthesized activators

Out of the twelve DHPs (Table 2) that we synthesized and evaluated for their biological activities, we took the best five compounds (**7a**, **7b**, **7c**, **7g** and **7i**) for our theoretical calculations. The geometries of these five ligands were refined using the LigPrep module (Schrödinger, Inc.). All possible ionization states and tautomers were generated at target pH 7 ± 2 . Since our ligand molecules contain chiral centers, we also generated various chirality combinations in order to see which enantiomeric form provides the best binding results. After generating all possible ionization states, tautomers and stereoisomers, our ligand library comprised of a total of eight states, i.e., seven states of the best five compounds obtained after LigPrep refinement, plus one reference compound, (S)-BAY K 8644.

Step 2: Protein preparation and identification of binding site

The structure of KVAP-33H1 FV complex (PDB ID: 2A0L) was downloaded from the RCSB Protein Data Bank (www.rcsb.in) and refined for our further calculations using the protein preparation workflow in Schrödinger. The imported protein is a multimeric chain containing monoclonal fragments of FV chains, which were deleted, and the protein chains (A and B) of KVAP were retained. Employing the OPLS-2005 force field [36], the resultant structure was minimized until the root-mean-square deviation (RMSD) reached a maximum cutoff of 0.30 Å. This prepared protein, along with its well-known activator (S)-BAY K 8644, was used for finding the probable binding sites using the SiteMap module [37] developed by Schrödinger, Inc. SiteMap is Schrödinger's program for identifying and characterizing ligand binding sites. Various possible binding states were predicted by SiteMap, and based on their Site score and other important parameters, the active site was found to be at the interface of the two chains (A and B) of KVAP. The point to note here is that this is the same site as that of binding of its inhibitor.

Step 3: Glide docking

After ensuring that the protein and the ligand were in the correct form for docking, a receptor grid was generated using an advanced molecular docking program, Glide. A grid box of

size $80 \times 80 \times 80 \text{ \AA}^3$ with coordinates $X = 24.9501 \text{ \AA}$, $Y = 41.5458 \text{ \AA}$ and $Z = -8.5647 \text{ \AA}$ was generated at the centroid of the ligand. To gain insight into the protein–ligand complex, all the ligands prepared above were docked into the active site using the “extra precision” XP algorithm. The docking algorithm in Glide utilizes the OPLS-2005 molecular mechanics potential energy function for the final minimization.

Predicted off-target pharmacology

The off-target pharmacology of molecules from this work was predicted with CT-link [32,33]. Using as input two-dimensional chemical structures, CT-link applies ligand-based methods to predict the binding affinity of small molecules to a list of 3492 proteins for which pharmacological data are available in the public domain [34]. The five independent ligand-based methods implemented in CT-link version 2016 include descriptor-based similarity approaches [32,38], fuzzy fragment-based mapping [35], and target cross-pharmacology [36]. Detailed information on those methods is provided elsewhere [32,33,38,39]. The results from CT-link have been validated prospectively in a variety of applications [40–44].

Binding at human androgen receptor

Assays were carried out at endogenous androgen receptor expressed at T47D cell line [45]. Briefly 3×10^5 cells/well were seeded in a poly-D-lysine-treated 24-well plate in RPMI-1640 medium supplemented with 10% FBS and maintained at 37°C in a 5% CO_2 atmosphere for 24 h. Medium was replaced by assay medium containing RPMI-1640, 0.1% BSA, $1 \mu\text{M}$ Triamcinolone, 2 nM [^3H]R1881 and the test compounds. Cells were incubated for 2 h at 37°C and then washed twice with HBSS at 4°C . Then $500 \mu\text{L}$ of HBSS containing 0.5% sodium dodecyl sulfate and 20% glycerol were added to all the wells. $350 \mu\text{L}$ was transferred to a scintillation vial, and radioactivity was measured in a Beckman LS6500 scintillation detector. Nonspecific binding was defined with $100 \mu\text{M}$ testosterone.

CYP3A4 inhibition

Activity of the compounds at human CYP3A4 inhibition was measured by using Vivid fluorogenic cytochrome inhibition kit from Invitrogen following supplier recommendations.

Radioligand binding assays

Radioligand binding competition assays were performed in vitro using A1, A2A, A2B and A3 human receptors expressed in transfected CHO (*hA1*), HeLa (*hA2A* and *hA3*) and HEK-293 (*hA2B*) cells [46].

Acknowledgements This work was partially supported by Chem-Biobank, the Chemical Biology infrastructure initiative in Spain, carrying out the predictive and the biological activity of the synthesized compounds. The authors would like to thank CDRI, Lucknow, for carrying out the *in vivo* studies, Defence Research and Development Organization (DRDO) for financial support and University of Delhi, Delhi, for providing the laboratory and instrumentation facility.

References

- Carafoli E, Klee C (1999) Calcium as cellular regulator. Oxford University Press, New York, pp 171–200
- William JE, Venkata CSR (2011) Calcium channel blockers. *J Clin Hypertens* 13:687–689. doi:10.1111/j.1751-7176.2011.00513
- Bossert F, Meyer H, Wehinger E (1981) 4-Aryldihydropyridines, a new class of highly active calcium antagonists. *Angew Chem Int Edit* 20:762–769. doi:10.1002/anie.198107621
- Sohal HS, Goyal A, Sharma R, Khare R (2014) One-pot multicomponent synthesis of symmetrical Hantzsch 1,4-dihydropyridine derivatives using glycerol as clean and green solvent. *Eur J Med Chem* 5:171–175. doi:10.5155/eurjchem.5.1.171-175.943
- Ali HI, Ashida N, Nagamatsu T (2007) Design, synthesis, antitumor activity, and molecular docking study of novel 2-methylthio-, 2-amino-, and 2-(*N*-substituted amino)-10-alkyl-2-deoxo-5-deazaflavins. *Bioorg Med Chem* 15:6336–6352. doi:10.1016/j.bmc.2007.06.058
- Pavani MG, Nunez M, Brigidi P, Vitali B, Gambari R (2002) Antimicrobial and antitumor activity of *N*-heteroimine-1,2,3-dithiazoles and their transformation in triazolo-, imidazo-, and pyrazolopyrimidines. *Bioorg Med Chem* 10:449–456. doi:10.1016/S0968-0896(01)00294-2
- Sondhi SM, Johar M, Rajvanshi S, Dastidar SG, Shukla R, Raghuraj R, Lown JW (2001) Anticancer, anti-inflammatory and analgesic activity evaluation of heterocyclic compounds synthesized by the reaction of 4-isothiocyanato-4-methylpentan-2-one with substituted *o*-phenylenediamines, *o*-diaminopyridine and (Un)substituted. *Aust J Chem* 54:69–74. doi:10.1071/CH00141
- Narayana LB, Rao RRA, Rao SP (2009) Synthesis of new 2-substituted pyrido[2,3-*d*]pyrimidin-4(1H)-ones and their antibacterial activity. *Eur J Med Chem* 44:1369–1376. doi:10.1016/j.ejmech.2008.05.025
- Trivedi A, Dodiya D, Dholaria B, Kataria V, Bhuvu V, Shah V (2011) Synthesis and biological evaluation of some novel 1,4-dihydropyridines as potential antitubercular agents. *Chem Biol Drug Des* 78:881–886. doi:10.1111/j.1747-0285.2011.01233.x
- Shishoo CJ, Shirsath VS, Rathod IS, Patil MJ, Bhargava SS (2001) Design, synthesis and antihistaminic (H1) activity of some condensed 2-(substituted) arylaminoethylpyrimidine-4-(3H)-ones. *Arzneim Forsch* 51:221–231
- Jiang J, Rhee MA, Melman N, Ji X, Jacobson KA (2006) 6-Phenyl-1,4-dihydropyridine derivatives as potent and selective A3 adenosine receptor antagonists. *J Med Chem* 39:4667–4675. doi:10.1021/jm960457c
- Li AH, Chang L, Ji X, Melman N, Jacobson KA (2009) Functionalized congeners of 1,4-dihydropyridines as antagonist molecular probes for A3 adenosine receptors. *Bioconjug Chem* 10:667–677. doi:10.1021/bc9900136
- Bakali JE, Gilleron P, Malapel MB, Mansouri R, Muccioli GG, Djouina M, Barczyk A, Klupsch F, Andrzejak V, Lipka E, Furman C, Lambert DM, Chavatte P, Desreumaux P, Millet R (2012) 4-Oxo-1,4-dihydropyridines as selective CB2 cannabinoid receptor ligands. Part 2: Discovery of new agonists endowed with protective effect against experimental colitis. *J Med Chem* 55:8948–8952. doi:10.1021/jm3008568
- Nantermet PG, Barrow JC, Selnick HG, Homnick CF, Freidinger RM, Chang RS, O'Malley SS, Reiss DR, Broten TP, Ransom RW, Pettibone DJ, Olah T, Forray C (2000) Selective α 1a adrenergic receptor antagonists based on 4-aryl-3,4-dihydropyridine-2-ones. *Bioorg Med Chem Lett* 10:1625–1628. doi:10.1016/S0960-894X(99)00696-4
- Niwa T, Shiraga T, Hashimoto T, Kagayama A (2004) Effect of Nilvadipine, a dihydropyridine calcium antagonist, on cytochrome P450 activities in human hepatic microsomes. *Biol Pharm Bull* 27:415–417. doi:10.1248/bpb.27.415
- Viegas-Junior C, Danuello A, Silva DBV, Barreiro EJ, Fraga CA (2007) Molecular hybridization: a useful tool in the design of new drug prototypes. *Curr Med Chem* 14:1829–1829. doi:10.2174/092986707781058805
- Huang LJ, Hour MJ, Teng CM, Kuo SC (1992) Synthesis and antiplatelet activities of *N*-arylmethyl-3,4-dimethylpyrano[2,3-*c*]pyrazol-6-one derivatives. *Chem Pharm Bull* 40:2547–2551
- Mohamed NR, Khaireldin NY, Fahmy AF, El-Sayed AAF (2010) Facile synthesis of fused nitrogen containing heterocycles as anticancer agents. *Der Pharm Chem* 2:400–417
- Ueda T, Mase H, Oda N, Ito I (1981) Synthesis of pyrazolone derivatives. XXXIX. Synthesis and analgesic activity of pyrano[2,3-*c*]pyrazoles. *Chem Pharm Bull* 29:3522–3528. doi:10.1248/cpb.29.3522
- Kuo SC, Huang LJ, Nakamura H (1984) Synthesis and analgesic and antiinflammatory activities of 3,4-dimethylpyrano[2,3-*c*]pyrazol-6-one derivatives. *J Med Chem* 27:539–544. doi:10.1021/jm00370a020
- Assiery SE, Sayed GH, Fouda A (2004) Synthesis of some new annulated pyrazolo-pyrido (or pyrano) pyrimidine, pyrazolopyridine and pyranopyrazole derivatives. *Acta Pharma* 54:143–150
- Mohammad MM, Mohammad RJ, Mohammad B (2006) Facile synthesis of pyrano[2,3-*c*]pyrazol-6-one derivatives under microwave irradiation in solvent-free conditions. *Synth Comm* 36:51–58. doi:10.1080/00397910500328886
- Noda M, Shimizu S, Tanabe T, Takai T, Kayano T, Ikeda T, Takahashi H, Nakayama H, Kanaoka Y, Minamino N (1984) Primary structure of electrophorus electricus sodium channel deduced from cDNA sequence. *Nature* 312:121–127. doi:10.1038/312121a0
- Tanabe T, Takeshima H, Mikami A, Flockerzi V, Takahashi H, Kanqawa A, Kojima M, Matsuo H, Hirose T, Numa S (1987) Primary structure of the receptor for calcium channel blockers from skeletal muscle. *Nature* 328:313–318. doi:10.1038/328313a0
- Tempel BL, Papazian DM, Schwarz TL, Jan LY, Jan YN (1987) Sequence of a probable potassium channel component encoded at Shaker locus of *Drosophila*. *Science* 237:770–775. doi:10.1126/science.2441471
- Friesner RA, Banks JL, Murphy RB, Halgren TA, Klicic JJ, Mainz DT, Repasky MP, Knoll EH, Shelley M, Perry JK, Shaw DE, Francis P, Shenkin PS (2004) Glide: a new approach for rapid, accurate docking and scoring. 1. Method and assessment of docking accuracy. *J Med Chem* 47:1739–1749. doi:10.1021/jm0306430
- Halgren TA, Murphy RB, Friesner RA, Beard HS, Frye LL, Pollard WT, Banks JL (2004) Glide: a new approach for rapid, accurate docking and scoring. 2. Enrichment factors in database screening. *J Med Chem* 47(7):1750–1759. doi:10.1021/jm030644s
- Halgren TA (2009) Identifying and characterizing binding sites and assessing druggability. *J Chem Inf Model* 49(2):377–389. doi:10.1021/ci800324m
- Tikhonov DB, Zhorov BS (2005) Modeling P-loops domain of sodium channel: homology with potassium channels and interaction with ligands. *Biophys J* 88:184–197. doi:10.1529/biophysj.104.048173
- Tikhonov DB, Zhorov BS (2008) Molecular modeling of benzothiazepine binding in the L-type calcium channel. *J Biol Chem* 283:17594–17604. doi:10.1074/jbc.M800141200

31. Yamaguchi S, Zhorov BS, Yoshioka K, Nagao T, Ichijo H, Adachi-Akahane S (2003) Key roles of Phe1112 and Ser1115 in the pore-forming IIS5–S6 linker of L-type Ca^{2+} channel $\alpha_1\text{C}$ subunit (CaV 1.2) in binding of dihydropyridines and action of Ca^{2+} channel agonists. *Mol Pharmacol* 64:235–248. doi:[10.1124/mol.64.2.235](https://doi.org/10.1124/mol.64.2.235)
32. Vidal D, Garcia-Serna R, Mestres J (2011) Ligand-based approaches to in silico pharmacology. *Methods Mol Biol* 672:489–502. doi:[10.1007/978-1-60761-839-3_19](https://doi.org/10.1007/978-1-60761-839-3_19)
33. Garcia-Serna R, Vidal D, Remez N, Mestres J (2015) Large-scale predictive drug safety: from structural alerts to biological mechanisms. *Chem Res Toxicol* 28:1875–1887. doi:[10.1021/acs.chemrestox.5b00260](https://doi.org/10.1021/acs.chemrestox.5b00260)
34. Gaulton A, Hersey A, Nowotka M, Bento AP, Chambers J, Mendez D, Motow P, Atkinson F, Bellis LJ, Cibrián-Uhalte E, Davies M, Dedman N, Karlsson A, Magariños MP, Overington JP, Papadatos G, Smit I, Leach AR (2017) The ChEMBL database in 2017. *Nucleic Acids Res* 45:D945–D954. doi:[10.1093/nar/gkw1074](https://doi.org/10.1093/nar/gkw1074)
35. Matsui T, Takeuchi M, Yamagishi S (2010) Nifedipine, a calcium channel blocker, inhibits inflammatory and fibrogenic gene expressions in advanced glycation end product (AGE)-exposed fibroblasts via mineralocorticoid receptor antagonistic activity. *Biochem Biophys Res Commun* 396:566–570. doi:[10.1016/j.bbrc.2010.04.149](https://doi.org/10.1016/j.bbrc.2010.04.149)
36. Jorgensen WL, Maxwell DS, Tirado-Rives J (1996) Development and testing of the OPLS all-atom force field on conformational energetics and properties of organic liquids. *J Am Chem Soc* 118:11225–11236. doi:[10.1021/ja9621760](https://doi.org/10.1021/ja9621760)
37. SiteMap (2009) version 2.3, Schrödinger. LLC, New York, NY
38. Keiser MJ, Roth BL, Armbruster BN, Ernsberger P, Irwin JJ, Shoichet BK (2007) Relating protein pharmacology by ligand chemistry. *Nat Biotechnol* 25:197–206. doi:[10.1038/nbt1284](https://doi.org/10.1038/nbt1284)
39. Briansó F, Carrascosa MC, Oprea TI, Mestres J (2011) Cross-pharmacology analysis of G protein-coupled receptors. *Curr Top Med Chem* 11:1956–1963. doi:[10.2174/156802611796391285](https://doi.org/10.2174/156802611796391285)
40. Areias FM, Brea J, Gregori-Puigjané E, Zaki MEA, Carvalho MA, Domínguez E, Gutiérrez-de-Terán H, Proença MF, Loza MI, Mestres J (2010) In silico directed chemical probing of the adenosine receptor family. *Bioorg Med Chem* 18:3043–3052. doi:[10.1016/j.bmc.2010.03.048](https://doi.org/10.1016/j.bmc.2010.03.048)
41. Mestres J, Seifert SA, Oprea TI (2011) Linking pharmacology to clinical reports: cyclobenzaprine and its possible association with serotonin syndrome. *Clin Pharmacol Ther* 90:662–665. doi:[10.1021/clpt.2011.177](https://doi.org/10.1021/clpt.2011.177)
42. Antolín AA, Jalencas X, Yélamos J, Mestres J (2012) Identification of PIM kinases as novel targets for PJ34 with confounding effects in PARP biology. *ACS Chem Biol* 7:1962–1967. doi:[10.1021/cb300317y](https://doi.org/10.1021/cb300317y)
43. Antolín AA, Mestres J (2015) Distant polypharmacology among MLP chemical probes. *ACS Chem Biol* 10:395–400. doi:[10.1021/cb500393m](https://doi.org/10.1021/cb500393m)
44. Montolio M, Gregori-Puigjané E, Pineda D, Mestres J, Navarro P (2012) Identification of small molecule inhibitors of amyloid β -induced neuronal apoptosis acting through the imidazoline I(2) receptor. *J Med Chem* 55:9838–9846. doi:[10.1021/jm301055g](https://doi.org/10.1021/jm301055g)
45. Waller CL, Juma BW, Gray LE Jr, Kelce WR (1996) Three-dimensional quantitative structure-activity relationships for androgen receptor ligands. *Toxicol Appl Pharmacol* 137:219–227. doi:[10.1006/taap.1996.0075](https://doi.org/10.1006/taap.1996.0075)
46. Stefanachi A, Nicolotti O, Leonetti F, Cellamare S, Campagna F, Loza MI, Brea JM, Mazza F, Gavuzzo E, Carotti A (2008) 1,3-Dialkyl-8-(hetero)aryl-9-OH-9-deazaxanthines as potent A2B adenosine receptor antagonists: design, synthesis, structure-affinity and structure-selectivity relationships. *Bioorg Med Chem* 16:9780–9789. doi:[10.1016/j.bmc.2008.09.067](https://doi.org/10.1016/j.bmc.2008.09.067)